Supplementary Materials for

Structure of the intact C2S2-type Photosystem II-LHCII supercomplex from *Arabidopsis thaliana* at 2.44 Å

Jack Forsman[1,2†*], André Graça[1†], Abuzer Orkun Aydin[2], Michael Hall[1], Rana Hussein[3,4], Wolfgang P. Schröder[1,5*], Johannes Messinger[2,5*]

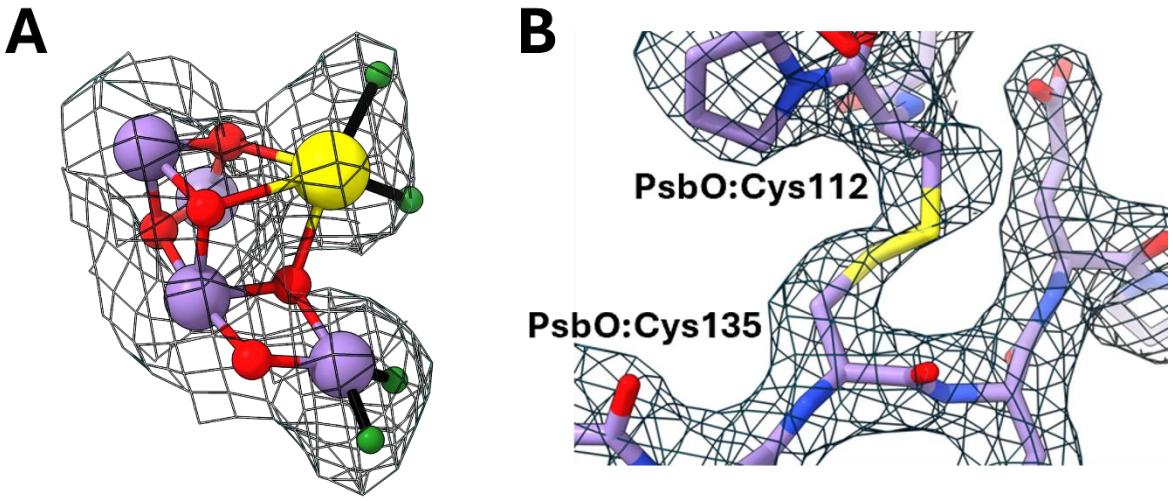

Supplementary Figure 1: (A) Mn_4CaO_5 cluster and ligated waters W1,W2,W3 and W4 from the current Arabidopsis structure. Manganese atoms are shown as purple spheres, the calcium atom is shown as a yellow sphere, and the oxo-bridges are shown as red spheres. The ligated waters are shown as green spheres. The black mesh represents the Coulomb potential maps of the Mn_4CaO_5 cluster from the locally sharpened CryoEM map at a contour level of 1.29 RMSD. **(B)** A frequently damaged disulfide bond in the PsbO protein with the associated CryoEM map density that was largely intact in this structure. PsbO residues are shown as purple sticks with oxygen atoms shown in red, nitrogen atoms shown in blue, sulfur atoms are shown in yellow. The Coulomb potential map of the locally sharpened CryoEM map at a contour level of 1.5RMSD is shown as a black mesh.

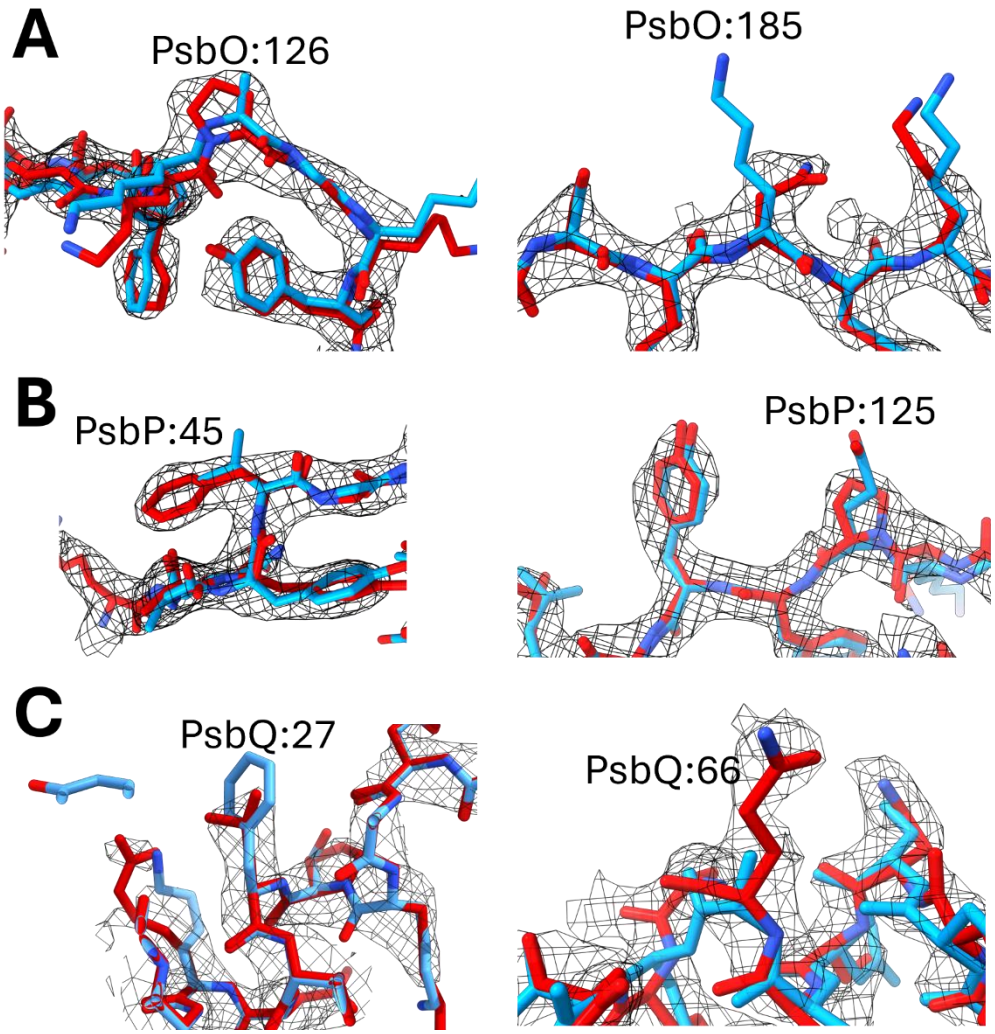

Supplementary Figure 2: Comparison of the different isoforms of PsbO, PsbP and PsbQ. Atomic models of PsbO1, PsbP1 and PsbQ1 (red) were aligned with atomic models of PsbO2, PsbP2 and PsbQ2 (blue) and fit into the locally sharpened Coulomb potential map at a contour level of 1.29 RMSD. **(A)** PsbO isoform comparison at position 126 and 185**,** this shows that the residues of PsbO1 fit the Coulomb potential map better than PsbO2. **(B)** PsbP isoform comparison at position 45 and 125**,** this shows the residues of PsbP1 fit the Coulomb potential map better than PsbP2. **(C)** PsbQ isoform comparison at position 27 and 66, this shows that the residues of PsbQ1 fit the Coulomb potential map better than PsbQ2.

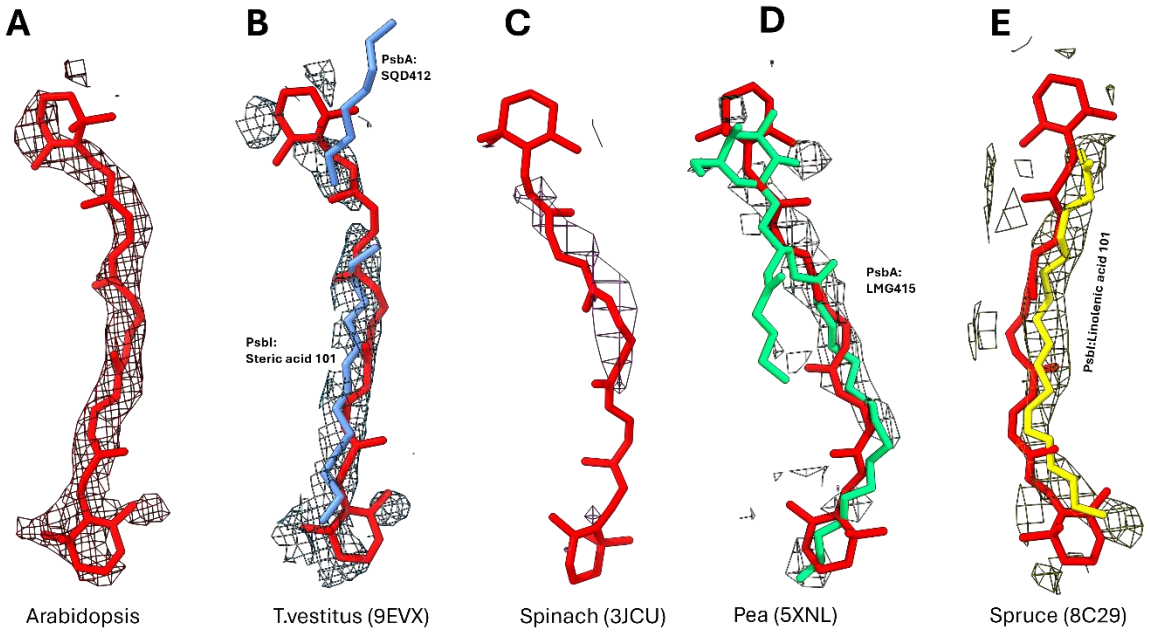

Supplementary Figure 3: CryoEM Coulomb potential maps of the area around the newly modelled β-carotene from *Arabidopsis thaliana* (locally sharpened map, contour level 1.38 RMSD) **(A)**, *T. vestitus* (9EVX and emd_50019, contour level 0.177 RMSD) **(B)**, spinach (3JCU and emd_6617, contour level 0.08 RMSD) **(C)**, pea (5XNL and emd_6741, contour level 16 RMSD) **(D)** and spruce (8C29 and emd_16389, contour level 0.988 RMSD) **(E).** The newly modelled β-carotene (red) is shown in each panel, with the electron density from the CryoEM maps from each species shown as a black mesh. For T. vestitus **(B)** there is a sulfoquinovosyl diacylglycerol (SQD) tail (blue) and a Steric acid (blue) modelled in this electron density. For spinach **(C)** there is nothing modelled. For pea **(D)** there is a distearoyl-monogalactosyl-diglyceride (LMG) (green) modelled into the Coulomb potential map. For spruce **(E)** there is a Linolenic acid (yellow) modelled in the Coulomb potential map.

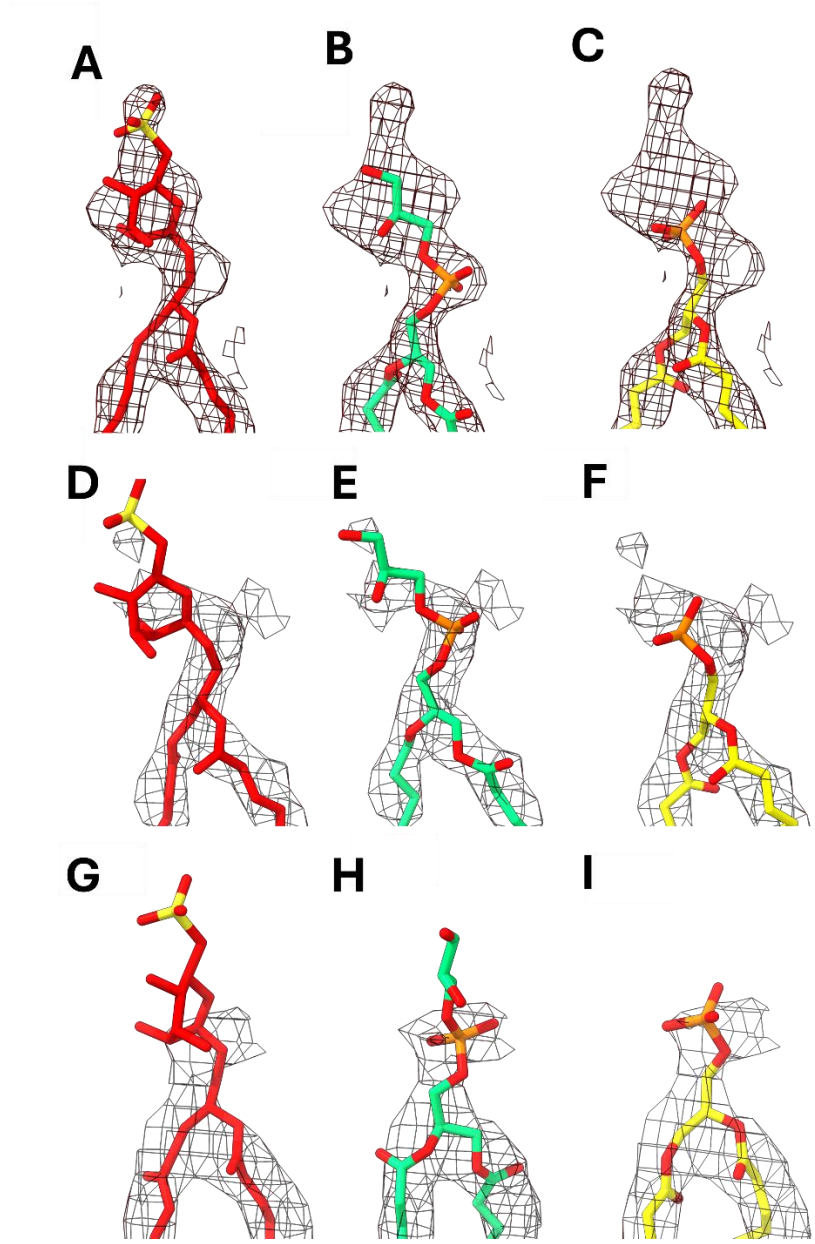

Supplementary Figure 4: Fitting of different ligands into the Coulomb potential maps at the interface between CP43 and the s-LHC II trimer in the Coulomb potential maps from different organisms. **(A-C)** Fitting of various ligands into the unsharpened (full) Coulomb potential map from the Arabidopsis (current structure) , contour level 1.62 RMSD. Fitting of **(A)** sulfoquinovosyl diacylglycerol (SQD) (ligand modelled in Arabidopsis, current structure) **(B)** dipalmitoyl-phosphatidyl-glycerol (LHG) (ligand modelled in pea, 5XNL), **(C)** Phosphatidic acid (3PH) (ligand modelled in spruce, 8C29). **(D-F)** Fitting of SQD **(D)**, LHG **(E)** and 3PH **(F)** into the Coulomb potential map found at the interface between CP43 and the s-LHC II trimer in the emd_6741 (pea) cryoEM map at contour level 16 RMSD. **(G-I)** Fitting of SQD **(G)**, LHG **(H)** and 3PH **(I)** into the Coulomb potential map found at the interface between CP43 and the s-LHC II trimer in the emd_16389 (spruce) Coulomb potential map at contour level 1 RMSD.

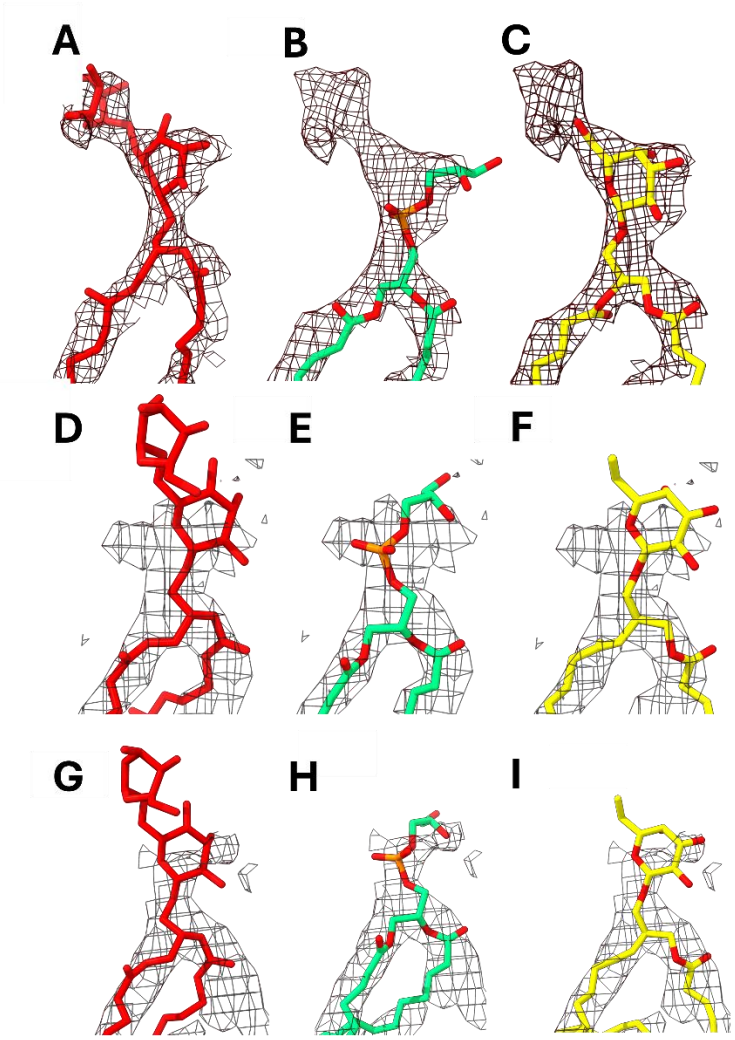

Supplementary Figure 5: Fitting of different ligands into the Coulomb potential maps at the interface between CP43 and the s-LHC II trimer in the cryoEM maps from different organisms. **(A-C)** Fitting of various ligands into the unsharpened (full) Coulomb potential map from the Arabidopsis (current structure) , contour level 1.62 RMSD. Fitting of **(A)** digalactosyl diacylglycerol (DGD) (ligand modelled in Arabidopsis, current structure) **(B)** dipalmitoyl-phosphatidyl-glycerol (LHG) (ligand modelled in pea, 5XNL), **(C)** distearoyl-monogalactosyl-diglyceride (LMG) (ligand modelled in spruce, 8C29). **(D-F)** Fitting of SQD **(D)**, LHG **(E)** and 3PH **(F)** into the Coulomb potential map found at the interface between CP43 and the s-LHC II trimer in the emd_6741 (pea) cryoEM map at contour level 16 RMSD. **(G-I)** Fitting of SQD **(G)**, LHG **(H)** and 3PH **(I)** into the Coulomb potential map found at the interface between CP43 and the s-LHC II trimer in the emd_16389 (spruce) Coulomb potential map at contour level 1 RMSD.

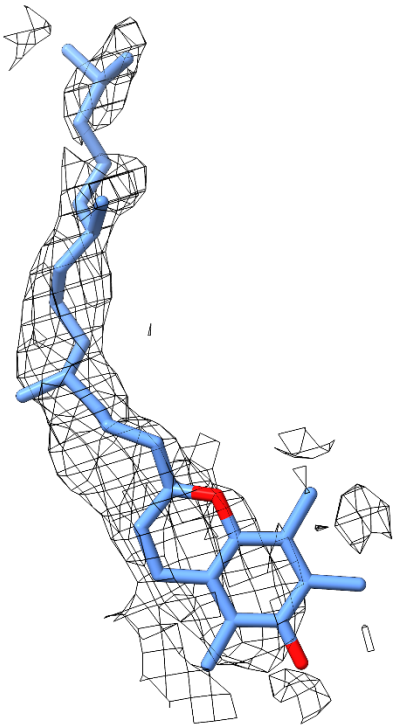

Supplementary Figure 6: Fitting of an α-tocopherol molecule into an unmodelled density in the unsharpened Coulomb potential map at a contour level of 0.3 RMSD. This unmodelled density is found at a similar position to where the α-tocopherol molecule is found in the spruce photosystem II model (8C29). Without confirmation of the presence of α-tocopherol in *Arabidopsis thaliana* the α-tocopherol molecule was not included in our model.

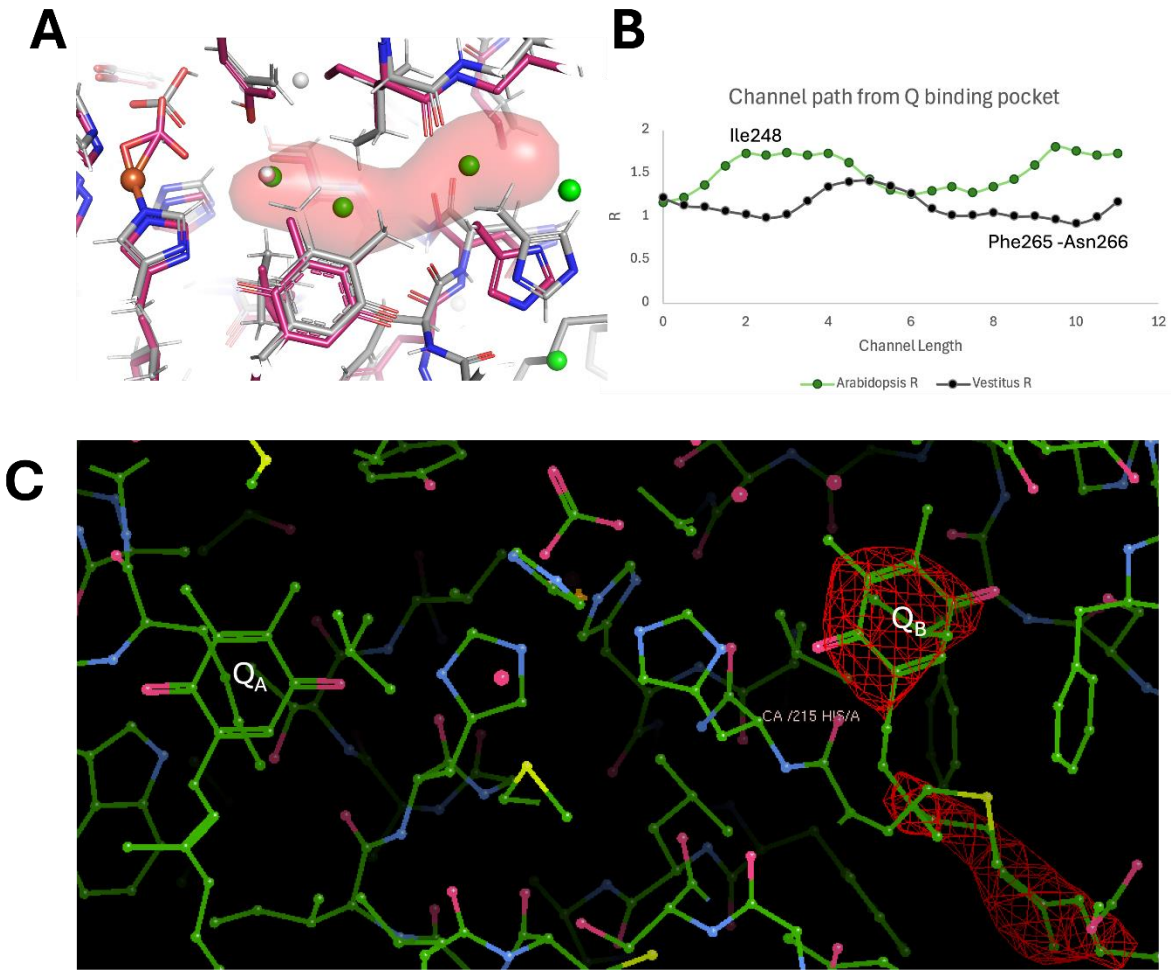

Supplementary Figure 7: A. A water channel can be calculated which connects the Q_B binding pocket to the stroma. The channel calculated in the Arabidopsis structure is shown in red. The Arabidopsis residues are shown as pink sticks, *T.vestitus* residues are shown as grey sticks. Red and blue sections indicate oxygen and nitrogen atoms, respectively. Waters from the Arabidopsis structure are shown as green spheres, waters from the *T.vestitus* structure are shown as white spheres. The non-heme iron is shown as an orange sphere. **B**. The radius along the calculated channel is shown for *Arabidopsis thaliana* (Green line) and *T. vestitus* (Black line). At points where the different species show large differences in the channel radius, the nearby D1 residues are labelled. This shows that in the *Arabidopsis thaliana* the water channel connecting the Q_B binding pocket to the protein exterior is wider on average than in *T. vestitus*. **C.** A difference map showing the difference between the current map, and a map where the B-factor of Q_B has been set to the same as Q_A. Q_A and Q_B are labelled. The red mesh indicates a negative density. This difference map demonstrates that Q_B has a reduced occupancy relative to Q_A in this Coulomb potential map.

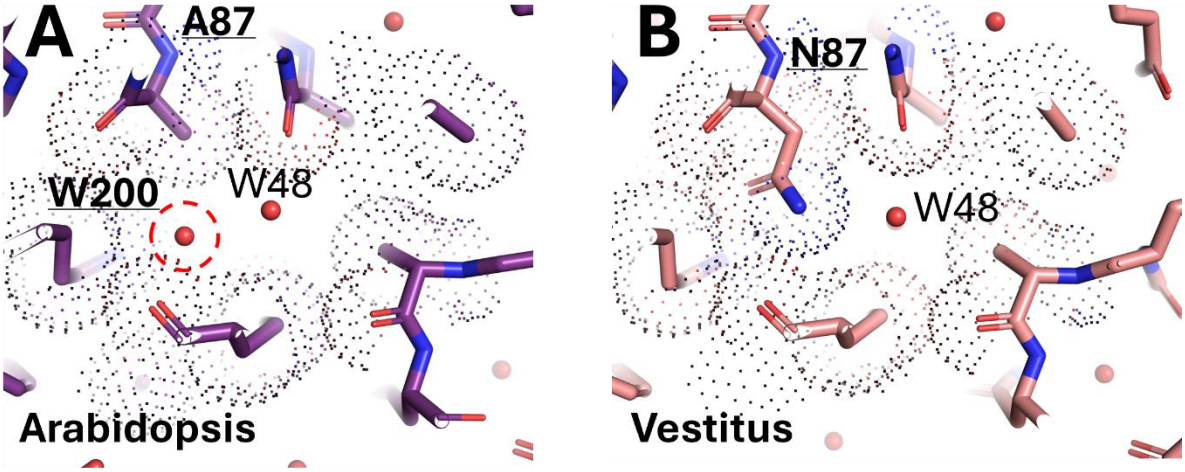

Supplementary Figure 8: View the amino acids surrounding the D1:87 residue in *Arabidopsis thaliana* (Panel A, current structure) and *T. vestitus* (Panel B, 9EVX) with a dotted van der Waals surface. The comparison shows how the substitution of the bulky asparagine to alanine creates space for W200, demonstrating why the W200 water is not detected *T. vestitus.*

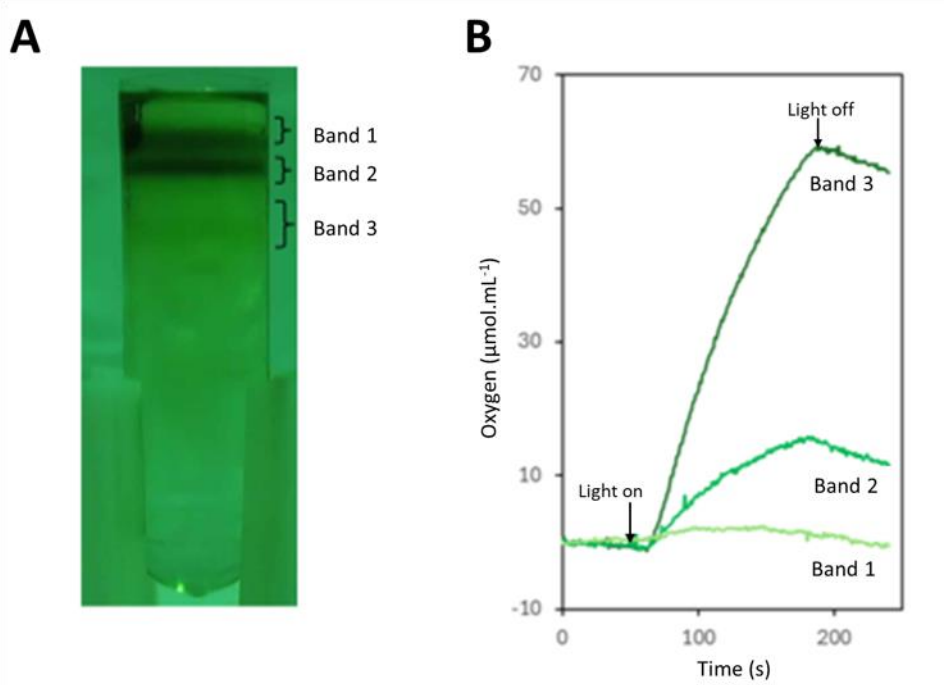

Supplementary Figure 9: A. 0.5 M sucrose gradient used to separate the β-DM solubilised protein complexes from *Arabidopsis thaliana* BBY membranes. **B.** Oxygen evolving activity of the different bands collected from the sucrose gradient. Oxygen evolution was measured at 10 µg Chl.mL^{-1} and supported using PPBQ and FeCN as electron acceptors. The initial rates of oxygen evolution for Band 1, Band 2 and Band 3 are 20, 75 and 240 µmol O_2.mgChl^{-1}.h^{-1}, respectively.

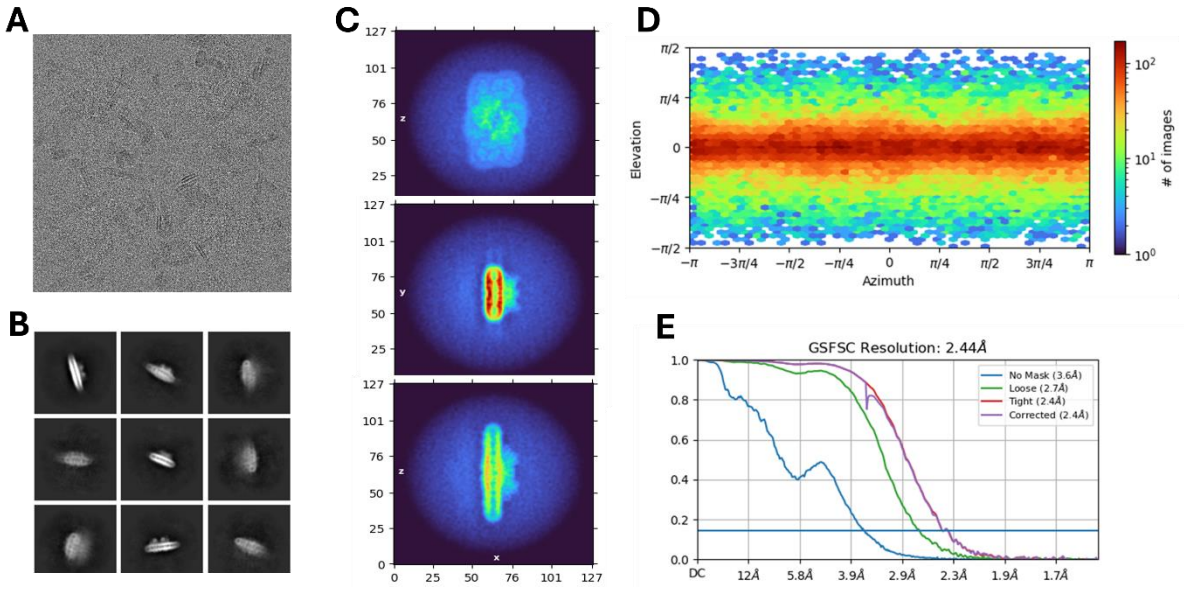

Supplementary Figure 10: Cryo-electron microscopy workflow. **A.** Example of one of the 16,450 micrographs collected. Micrographs were collected at 215,000 X magnification. **B.** Example of some of the 2D classes used to separate the 3,054,062 particles extracted from the micrographs into 322,522 "good particles". **C.** Example of the best class from Ab initio reconstruction. This class was formed from 72,301 particles. **D.** Distribution of the orientation of the particles used to generate the best class from Ab initio reconstruction. **E.** Gold standard FSC curve for the refined maps from the best class of Ab initio reconstruction (**C.**).

Supplementary Table 1: Statistics of cryo-EM data and structural analysis of the C2S2-type PSII supercomplex refined at 2.44 Å resolution.

Data collection and processing	
Hardware	
Microscope	Titan Krios
Detector (mode)	FEI Falcon IV
Voltage (keV)	300
Spherical aberration	2.7
Magnification	215,000 x
Electron exposure (e/Å^2)	40
Defocus range (μm)	-0.8 to -2.0 (0.2 increments)
Pixel size (Å)	0.5744
Symmetry imposed	C2
Initial particle images (no.)	3,054,062
Final particle images (no.)	72 301
Map resolution (Å)	2.44 (C_2S_2 - masked)
FSC threshold	0.143
Refinement	
Initial models used (PDB code)	3JCU
Model composition	
Non-hydrogen atoms	76841
Protein residues	7542
Ligands	334
Water molecules	1202
B factors (Å^2)	
Protein (mean)	160.9
Ligand (mean)	167.5
R.m.s. deviations	
Bond lengths (Å)	0.01
Bond angles (°)	1.24
Validation	
MolProbity score	2.27
Clash score	14.18
Rotamer outliers (%)	3.35
Ramachandran plot	
Favored (%)	96.61
Allowed (%)	3.22
Outliers (%)	0.16

Supplemental table 2: Details of the individual Photosystem II subunits. The protein name is shown in bold, while the gene name is contained within parenthesis. The accession code used to identify the protein in UniProt is shown before the sequence. The sequences have amino acids letters colored in red and black: **black** letters, all the amino acids that were modelled, **red**, amino acids that are not observed in a 3D map of Arabidopsis thaliana. Each subunit is shown fit into the local sharpened electron density map at a contour level of 1.5. Each subunit from the model is shown with red sticks. The electron density map surrounding the subunit within a distance of 2 Å is shown as a blue surface.

Chain ID	Protein Name (Gene name)	MW (kDa)	Sequence (mature protein)	Model fit into the electrostatic potential map
A,a	**D1** (PsbA)	37.98	>P83755 MTAILERRESESLWGRFCNWITSTENRLYI GWFGVLMIPTLLTATSVFIIAFIAAPPVDIDG IREPVSGSLLYGNNIISGAIIPTSAAIGLHFYP IWEAASVDEWLYNGGPYELIVLHFLLGVA CYMGREWELSFRLGMRPWIAVAYSAPVA AATAVFLIYPIGQGSFSDGMPLGISGTFNFM IVFQAEHNILMHPFHMLGVAGVFGGSLFSA MHGSLVTSSLIRETTENESANEGYRFGQEE ETYNIVAAHGYFGRLIFQYASFNNSRSLHFF LAAWPVVGIWFTALGISTMAFNLNGFNFN QSVVDSQGRVINTWADIINRANLGMEVMH ERNAHNFPLDLAA	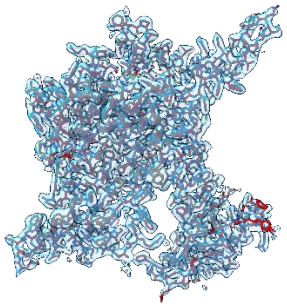
B,b	**CP47** (PsbB)	56.04	>P56777 MGLPWYRVHTVVLNDPGRLLAVHIMHTA LVAGWAGSMALYELAVFDPSDPVLDPMW RQGMFVIPFMTRLGITNSWGGWNITGGTIT NPGLWSYEGVAGAHIVFSGLCFLAAIWHW VYWDLEIFCDERTGKPSLDLPKIFGIHLFLS GVACFGFGAFHVTGLYGPGIWVSDPYGLT GKVQPVNPAWGVEGFDPFVPGGIASHHIA AGTLGILAGLFHLSVRPPQRLYKGLRMGNI ETVLSSSIAAVFFAAFVVAGTMWYGSATTP IELFGPTRYQWDQGYFQQEIYRRVSAGLAE NQSLSEAWAKIPEKLAFYDYIGNNPAKGGL FRAGSMDNGDGIAVGWLGHPVFRNKEGR ELFVRRMPTFFETFPVVLVDGDGIVRADVP FRRAESKYSVEQVGVTVEFYGGELNGVSY SDPATVKKYARRAQLGEIFELDRATLKSDG VFRSSPRGWFTFGHASFALLFFFGHIWHGA RTLFRDVFAGIDPDLDAQVEFGAFQKLGDP TTKRQAV	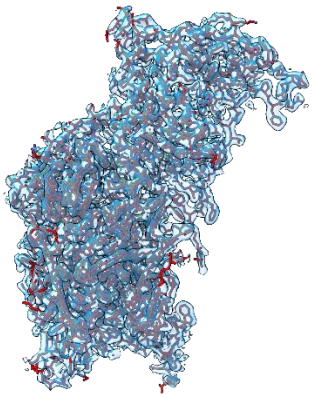
C,c	**CP43** (PsbC)	50.04	>P56778 TLFNGTLALAGRDQETTGFAWWAGNARLI NLSGKLLGAHVAHAGLIVFWAGAMNLFE VAHFVPEKPMYEQGLILLPHLATLGWGVG PGGEVIDTFPYFVSGVLHLISSAVLGFGGIY HALLGPETLEESFPFFGYVWKDRNKMTTIL GIHLILLGVGAFLLVFKALYFGGVYDTWAP GGGDVRKITNLTLSPSVIFGYLLKSPFGGEG WIVSVDDLEDIIGGHVWLGSICIFGGIWHIL TKPFAWARRALVWSGEAYLSYSLAALSVC GFIACCFVWFNNTAYPSEFYGPTGPEASQA QAFTFLVRDQRLGANVGSAQGPTGLGKYL MRSPTGEVIFGGETMRFWDLRAPWLEPLR GPNGLDLSRLKKDIQPWQERRSAEYMTHA PLGSLNSVGGVATEINAVNYVSPRSWLSTS HFVLGFFLFVGHLWHAGRARAAAAGFEK GIDRDFEPVLSMTPLN	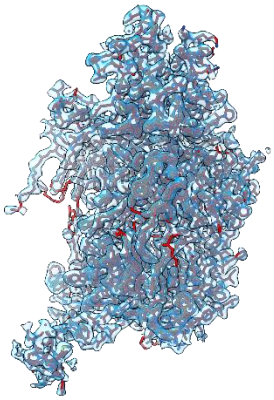

D,d	**D2** (PsbD)	39.42	>P56761 TIALGKFTKDEKDLFDIMDDWLRRDRFVF VGWSGLLLFPCAYFALGGWFTGTTFVTSW YTHGLASSYLEGCNFLTAAVSTPANSLAHS LLLLWGPEAQGDFTRWCQLGGLWAFVAL HGAFALIGFMLRQFELARSVQLRPYNAIAF SGPIAVFVSVFLIYPLGQSGWFFAPSFGVAA IFRFILFFQGFHNWTLNPFHMMGVAGVLG AALLCAIHGATVENTLFEDGDGANTFRAF NPTQAEETYSMVTANRFWSQIFGVAFSNK RWLHFFMLFVPVTGLWMSALGVVGLALN LRAYDFVSQEIRAAEDPEFETFYTKNILLNE GIRAWMAAQDQPHENLIFPEEVLPRGNAL	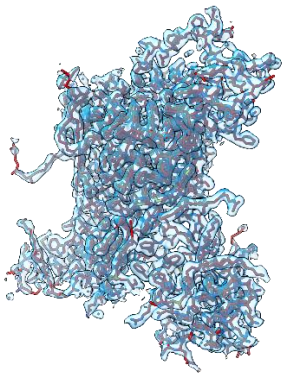
E,e	**Cytochrome $b_{559}\alpha$** (PsbE)	9.39	>P56779 MSGSTGERSFADIITSIRYWVIHSITIPSLFIA GWLFVSTGLAYDVFGSPRPNEYFTESRQGI PLITGRFDSLEQLDEFSRSF	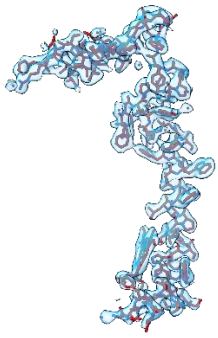
F,f	**Cytochrome $b_{559}\beta$** (PsbF)	4.42	>P62095 MTIDRTYPIFTVRWLAVHGLAVPTVFFLGSI SAMQFIQR	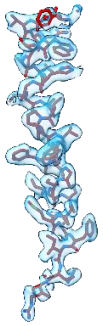
H,h	**Photosystem II reaction center protein H** (PsbH)	7.57	>P56780 ATQTVEDSSRSGPRSTTVGKLLKPLNSEYG KVAPGWGTTPLMGVAMALFAVFLSIILEIY NSSVLLDGISVN	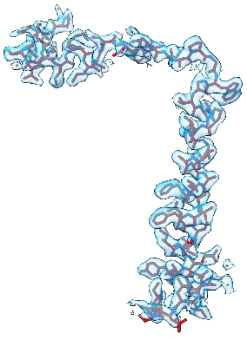

I,i	**Photosystem II reaction center protein I** (PsbI)	4.17	>P62100 MLTLKLFVYTVVIFFVSLFIFGFLSNDPGRN PGREE	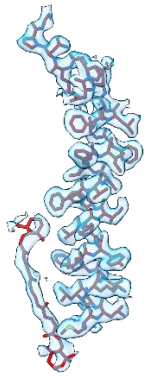
J,j	**Photosystem II reaction center protein J** (PsbJ)	4.12	>P56781 MADTTGRIPLWVIGTVAGILVIGLIGIFFYG SYSGLGSSL	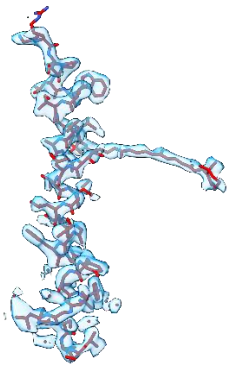
K,k	**Photosystem II reaction center protein K** (PsbK)	4.24	>P56782 KLPEAYAFLNPIVDVMPVIPLFFLLLAFVW QAAVSFR	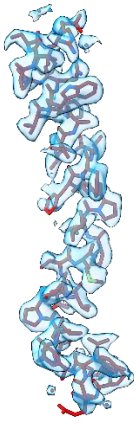
L,l	**Photosystem II reaction center protein L** (PsbL)	4.47	>P60129 MTQSNPNEQSVELNRTSLYWGLLLIFVLAV LFSNYFFN	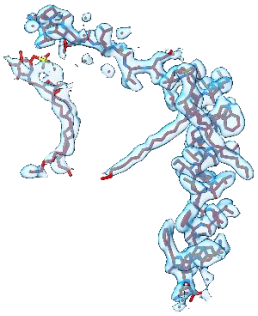

M,m	**Photosystem II reaction center protein M** (PsbM)	3.78	>P62109 MEVNILAFIATALFILVPTAFLLIIYVKTVSQ ND	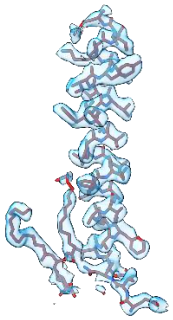
O,o	**Oxygen-evolving enhancer protein 1-1** (PsbO1)	26.57	>P23321 EGAPKRLTYDEIQSKTYMEVKGTGTANQC PTIDGGSETFSFKPGKYAGKKFCFEPTSFTV KADSVSKNAPPEFQNTKLMTRLTYTLDEIE GPFEVASDGSVNFKEEDGIDYAAVTVQLPG GERVPFLFTVKQLDASGKPDSFTGKFLVPS YRGSSFLDPKGRGGSTGYDNAVALPAGGR GDEEELVKENVKNTAASVGEITLKVTKSKP ETGEVIGVFESLQPSDTDLGAKVPKDVKIQ GVWYGQLE	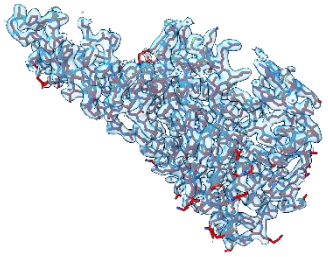
P,p	**Oxygen-evolving enhancer protein 2-1** (PsbP1)	28.10	>Q42029 MAYSACFLHQSALASSAARSSSSSSSQRHV SLSKPVQIICKAQQSHEDDNSAVSRRLALT LLVGAAAVGSKVSPADAAYGEAANVFGK PKTNTDFLPYNGDGFKVQVPAKWNPSKEI EYPGQVLRFEDNFDATSNLNVMVTPTDKK SITDYGSPEEFLSQVNYLLGKQAYFGETAS EGGFDNNAVATANILESSSQEVGGKPYYY LSVLTRTADGDEGGKHQLITATVNGGKLYI CKAQAGDKRWFKGARKFVESAATSFSVA	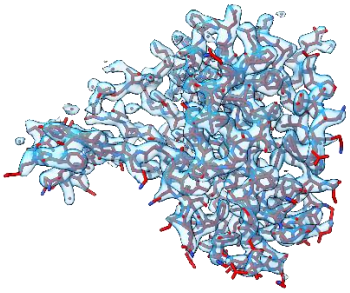
Q,q	**Oxygen-evolving enhancer protein 3-1** (PsbQ1)	23.87	>Q9XFT3 MASMGGLHGASPAVLEGSLKINGSSRLNG SGRVAVAQRSRLVVRAQQSEETSRRSVIGL VAAGLAGGSFVQAVLADAISIKVGPPPAPS GGLPAGTDNSDQARDFALALKDRFYLQPL PPTEAAARAKESAKDIINVKPLIDRKAWPY VQNDLRSKASYLRYDLNTIISSKPKDEKKS LKDLTTKLFDTIDNLDYAAKKKSPSQAEKY YAETVSALNEVLAKLG	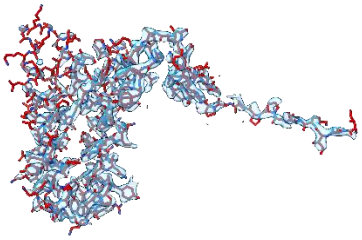

T,t	**Photosystem II reaction center protein Tc** (PsbTc)	3.82	>P61839 MEALVYTFLLVSTLGIIFFAIFFREPPKISTK K	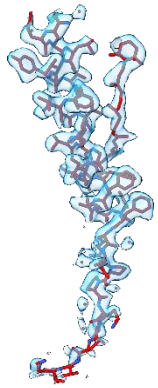
U,u	**Photosystem II reaction center protein Tn** (PsbTn)	3.17	>Q39195 EPKRGTEAAKKKYAQVCVTMPTAKICRY	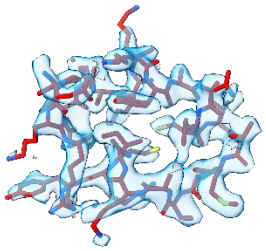
W,w	**Photosystem II reaction center W protein** (PsbW)	6.04	>Q39194 LVDERMSTEGTGLPFGLSNNLLGWILFGVF GLIWTFFFVYTSSLEEDEESGLSL	
X,x	**Photosystem II reaction center protein X** (PSII-X)	4.18	>Q9SKI3 AGSGISPSLKNFLLSIASGGLVLTVIIGVVVG VSNFDPVKRT	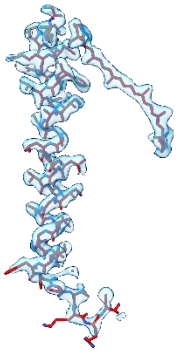

Z,z	**Photosystem II reaction center protein Z** (PsbZ)	6.57	>P56790 MTIAFQLAVFALIITSSILLISVPVVFASPDG WSSNKNVVFSGTSLWIGLVFLVGILNSLIS	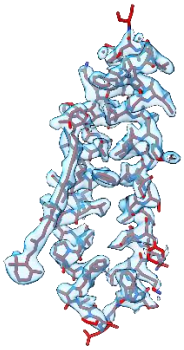
G,g	**Chlorophyll a-b binding protein 1 (**LHCB1.3)	24.86	>P04778 RKTVAKPKGPSGSPWYGSDRVKYLGPFSG ESPSYLTGEFPGDYGWDTAGLSADPETFAR NRELEVIHSRWAMLGALGCVFPELLARNG VKFGEAVWFKAGSQIFSDGGLDYLGNPSL VHAQSILAIWATQVILMGAVEGYRVAGNG PLGEAEDLLYPGGSFDPLGLATDPEAFAEL KVKELKNGRLAMFSMFGFFVQAIVTGKGPI ENLADHLADPVNNNAWAWAFTN	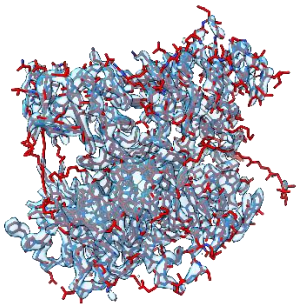
N,n	**Chlorophyll a-b binding protein 1 (**LHCB1.3)	24.86	>P04778 RKTVAKPKGPSGSPWYGSDRVKYLGPFSG ESPSYLTGEFPGDYGWDTAGLSADPETFAR NRELEVIHSRWAMLGALGCVFPELLARNG VKFGEAVWFKAGSQIFSDGGLDYLGNPSL VHAQSILAIWATQVILMGAVEGYRVAGNG PLGEAEDLLYPGGSFDPLGLATDPEAFAEL KVKELKNGRLAMFSMFGFFVQAIVTGKGPI ENLADHLADPVNNNAWAWAFTN	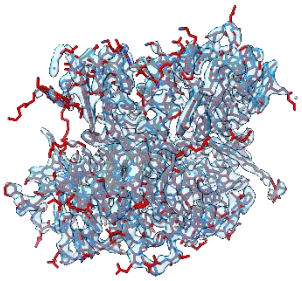
Y,y	**Chlorophyll a-b binding protein 1 (**LHCB1.3)	24.86	>P04778 RKTVAKPKGPSGSPWYGSDRVKYLGPFSG ESPSYLTGEFPGDYGWDTAGLSADPETFAR NRELEVIHSRWAMLGALGCVFPELLARNG VKFGEAVWFKAGSQIFSDGGLDYLGNPSL VHAQSILAIWATQVILMGAVEGYRVAGNG PLGEAEDLLYPGGSFDPLGLATDPEAFAEL KVKELKNGRLAMFSMFGFFVQAIVTGKGPI ENLADHLADPVNNNAWAWAFTN	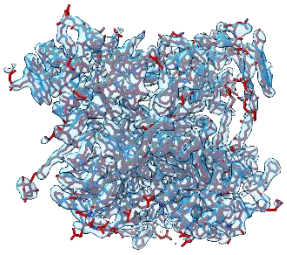

R,r	**CP29** (LHCB4.2)	28.16	>Q07473 AAPKKSAKKTVTTDRPLWYPGAISPDWLD GSLVGDYGFDPFGLGKPAEYLQFDIDSLDQ NLAKNLAGDVIGTRTEAADAKSTPFQPYSE VFGIQRFRECELIHGRWAMLATLGALSVE WLTGVTWQDAGKVELVDGSSYLGQPLPFS ISTLIWIEVLVIGYIEFQRNAELDSEKRLYPG GKFFDPLGLAADPEKTAQLQLAEIKHARLA MVAFLGFAVQAAATGKGPLNNWATHLSD PLHTTIIDTFSSS	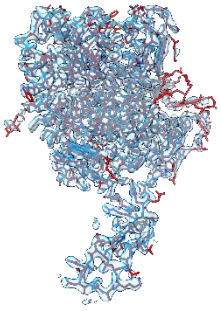
S,s	**CP26** (LHCB5)	25.21	>Q9XF89 SKAVSETSDELAKWYGPDRRIFLPDGLLDR SEIPEYLNGEVAGDYGYDPFGLGKKPENFA KYQAFELIHARWAMLGAAGFIIPEALNKY GANCGPEAVWFKTGALLLDGNTLNYFGK NIPINLVLAVVAEVVLLGGAEYYRITNGLD FEDKLHPGGPFDPLGLAKDPEQGALLKVK EIKNGRLAMFAMLGFFIQAYVTGEGPVENL AKHLSDPFGNNLLTVIAGTAERAPTL	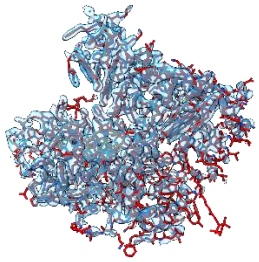

Supplemental table 3: Details of various ligands found within the structure.

Ligand Name	3-letter Code	# of ligands (full dimer)
β-CAROTENE	BCR	24
BICARBONATE ION	BCT	2
CHLOROPHYLL B	CHL	50
CHLORIDE ION	CL	4
CHLOROPHYLL A	CLA	156
DIGALACTOSYL DIACYL GLYCEROL (DGDG)	DGD	10
FE (II) ION	FE2	2
PROTOPORPHYRIN IX CONTAINING FE	HEM	2
WATER	HOH	1202
1,2-DIPALMITOYL-PHOSPHATIDYL-GLYCEROLE	LHG	18
1,2-DISTEAROYL-MONOGALACTOSYL-DIGLYCERIDE	LMG	10
DODECYL-BETA-D-MALTOSIDE	LMT	2
(3R,3'R,6S)-4,5-DIDEHYDRO-5,6-DIHYDRO-BETA,BETA-CAROTENE-3,3'-DIOL	LUT	18
(3S,5R,6R,3'S,5'R,6'S)-5',6'-EPOXY-6,7-DIDEHYDRO-5,6,5',6'-TETRAHYDRO-BETA,BETA-CAROTENE-3,5,3'-TRIOL; 9'-CIS-NEOXANTHIN	NEX	10
CA-MN4-O5 CLUSTER	OEX	2
PHEOPHYTIN A	PHO	4
2,3-DIMETHYL-5-(3,7,11,15,19,23,27,31,35-NONAMETHYL-2,6,10,14,18,22,26,30,34-HEXATRIACONTANONAENYL-2,5-CYCLOHEXADIENE-1,4-DIONE-2,3-DIMETHYL-5-SOLANESYL-1,4-BENZOQUINONE	PL9	4
1,2-DI-O-ACYL-3-O-[6-DEOXY-6-SULFO-ALPHA-D-GLUCOPYRANOSYL]-SN-GLYCEROL	SQD	8
(3S,5R,6S,3'S,5'R,6'S)-5,6,5',6'-DIEPOXY-5,6,5',6'-TETRAHYDRO-BETA,BETA-CAROTENE-3,3'-DIOL	XAT	8